ELSEVIER

Int. J. Therm. Sci. 41 (2002) 625–630

International Journal of Thermal Sciences

www.elsevier.com/locate/ijts

Condensation heat transfer coefficients of the zeotropic refrigerant mixture R-22/R-142b in smooth horizonal tubes ☆

F.J. Smit, J.P. Meyer *

Department of Mechanical and Aeronautical Engineering, University of Pretoria, Pretoria 002, South Africa

Received 29 October 2001; accepted 8 February 2002

Abstract

Heat transfer coefficients during condensation of the zeotropic refrigerant mixture R-22 with R-142b are presented. Measurements were obtained at different mass fractions in a smooth horizontal tube. All measurements were conducted at a high condensing saturation pressure of 2.43 MPa, which corresponds to a condensation temperature of 60 °C for R-22. The measurements were taken in 8.11 mm inner diameter smooth tubes with lengths of 1 603 mm. The heat transfer coefficients were determined with the Log Mean Temperature Difference equations. It was found that at low mass fluxes, between 40 $kg{\cdot}m^{-2}{\cdot}s^{-1}$ to 350 $kg{\cdot}m^{-2}{\cdot}s^{-1}$, the refrigerant mass fraction influences the heat transfer coefficient by up to a factor of two. The heat transfer coefficients decrease as the fraction of R-142b is increased. At high mass fluxes, of 350 $kg{\cdot}m^{-2}{\cdot}s^{-1}$ and more the heat transfer coefficients were not strongly influenced by the refrigerant mass fraction. The average heat transfer coefficient decreased by only 7% as the refrigerant mass fraction changed from 100% R-22 to 50%/50% R-22/R142b.

Keywords: Condensation; Mixtures; Tubes; R22; R142b

1. Introduction

It was agreed at the last follow-up conference held in Vienna in 1995, that the worldwide phase-out of hydrochlorofluorocarbons (HCFCs) as refrigerants in industrialised countries has to be fulfilled by 2030 and in developing countries by 2040 [1]. Manufacturers of air-conditioning and refrigeration equipment usually offer different refrigerants depending on where the manufacturer and customer are located. Manufacturers in Europe tend to offer R-134a for air-conditioning and natural refrigerants such as ammonia and propane for refrigeration and process cooling. Japanese manufacturers offer R-134a, R-404A and R-407C. In Thailand and China they offer R-22 ($CHClF_2$) units. Manufacturers in the USA offer many refrigerants, and although options are available, R-22 remains extremely popular.

In non-industrialised countries where air-conditioning, heat pump and refrigeration equipment are being developed, HCFCs are still being used for new equipment under development such as hot-water heat pumps heaters. Especially R-22 is very popular and it seems as if it will be used up to 2040 if allowed by legislation and the cost stays reasonable.

Hot-water heat pumps are especially used in countries with a mild climate in winter, that have no natural gas and where electrical heating is usually used for the heating of water. Heating of water with heat pumps is extremely energy-efficient. Savings of approximately 67% can be realised, compared to heating with direct electrical resistance heaters [2,3]. Hot-water heat pumps are vapour compression cycles, which use water-cooled condensers for the heating of hot water. The most widely used refrigerant for hot-water heat pumps is R-22 with which a maximum hot-water temperature of 60 °C to 65 °C is possible with approximately the same condensing temperatures. This is possible by making use of the refrigerant's superheat, which is approximately at 120 °C at the compressor outlet. The maximum condensation temperature is limited by the maximum condensing pressure to control the amount of wear in the compressor bearings, the load on the bearings, and to keep the lubrication oil from decomposing at higher compressor discharge temperatures.

☆ This article is a follow-up a communication presented by the authors at the ExHFT-5 (5th World Conference on Experimental Heat Transfer, Fluid Mechanics and Thermodynamics), held in Thessaloniki in September 24–28, 2001.

* Correspondence and reprints.
E-mail address: JPMeyer@postino.up.ac.za (J.P. Meyer).

1290-0729/02/$ – see front matter
PII: S1290-0729(02)01356-X

Nomenclature

A	area	m^2	
C_P	heating capacity at constant pressure	$J \cdot kg^{-1} \cdot °C^{-1}$	
h	enthalpy	$J \cdot kg^{-1}$	
h/HTC	heat transfer coefficient	$W \cdot m^{-2} \cdot °C^{-1}$	
k	thermal conductivity	$W \cdot m^{-1} \cdot °C^{-1}$	
L	length	m	
m	mass flow rate	$kg \cdot s^{-1}$	
P	pressure	Pa	
Q	heat transfer	W	
R	radius	m	
T	temperature	°C	
U	overall heat transfer coefficient	$W \cdot m^{-2} \cdot °C^{-1}$	
x	quality		
ρ	density	$kg \cdot m^{-3}$	
μ	viscosity	$Pa \cdot s^{-1}$	
σ	surface tention	$N \cdot m^{-1}$	

Subscripts

exp	experimental
f	liquid saturation point
g	vapour saturation point
i	inner or in-tube
in	inlet of test section
LMTD	logarithmic mean temperature difference
o	outer or annulus side
out	outlet of test section
pred	predicted
r	refrigerant
w	water

Although hot-water temperatures of 60 °C to 65 °C are adequate for domestic use, they are low when compared to temperatures that can be delivered by fossil fuel and direct electric resistance systems. This limits the potential applications of hot-water heat pumps. Smit and Meyer [4] as well as Johannsen [5] showed analytically that a zeotropic mixture of R-22 and R-142b ($CClF_2CH_3$) could be used to obtain higher temperatures. A hot-water outlet temperature of 120 °C is possible if only R-142b is used. The disadvantage of using only R-142b is that its heating capacity is 15% lower and its heating COP (coefficient of performance) is 7% lower when compared to R-22. Furthermore, it is flammable, but the flammability is decreased by adding R-22. A mixture of 60% R-22 with 40% R-142b to 80% R-22 with 20% R-142b by mass, is recommended. With these mixtures the heating capacities are about the same as just R-22, but its COP is increased while hot-water temperatures of 80 °C (80%/20% R-22/R-142b) to 90 °C (60%/40% R-22/R-142b) can be achieved. Mixtures of R-22 with R-142b form zeotropic mixtures with glides of 7 °C and 5 °C for 60% and 80% R-22, respectively.

Literature searches by Smit [6], Kebonte [7] and Bukasa [8] showed that apparently no literature on detailed heat transfer coefficients for the recommended mass fractions of R-22 with R-142b at a condensing temperature of 60 °C or more (condensing pressure of 2.43 MPa), has been published yet. In addition, it seems as if no detail condensation data exist for the mixture of R-22/R-142b. Meyer et al. [9] published an article on average condensation coefficients at this high condensing temperature but in the annulus of coiled tube-in-tube heat exchangers. Shizuya et al. [10] published an article on local heat transfer coefficients but only for a mole fraction ratio of 54/46.

The objective of this work was to determine heat transfer coefficients of the zeotropic mixture R-22 with R-142b at the following mass fractions: 90%/10%, 80%/20%, 70%/30%,

Table 1
Thermodynamic properties at different mass fractions of R-22/R-142b mixtures at a saturation pressure of 2.43 MPa

Mass fraction HCFC-22 [%]	100	90	80	70	60	50
T_f [°C]	60	63.23	66.64	70.53	74.64	79.10
T_g [°C]	60	65.72	71.07	76.13	80.97	85.64
Temperature glide [°C]	0	2.49	4.43	5.60	6.33	6.54
T_c [°C]	96.15	100.95	105.75	110.35	114.75	119.05
P_c [MPa]	4.990	5.0	4.988	4.954	4.899	4.822
ρ_f [$kg \cdot m^{-3}$]	1030	1013	995.6	977.7	959.5	940.8
ρ_g [$kg \cdot m^{-3}$]	111.6	110.8	110.7	111.0	111.8	112.9
μ_f [μPa·s]	107.6	107.2	106.5	105.5	104.2	102.6
μ_g [μPa·s]	14.97	14.94	14.88	14.81	14.73	14.65
h_{fg} [$kJ \cdot kg^{-1}$]	139.9	141.3	142.0	141.9	141.2	139.7
c_{pf} [$kJ \cdot kg^{-1} \cdot K^{-1}$]	1.539	1.548	1.561	1.578	1.598	1.624
c_{pg} [$kJ \cdot kg^{-1} \cdot K^{-1}$]	1.287	1.287	1.302	1.327	1.358	1.399
k_f [$W \cdot m^{-1} \cdot K^{-1}$]	0.06763	0.06641	0.06516	0.06389	0.06258	0.06125
k_g [$W \cdot m^{-1} \cdot K^{-1}$]	0.01636	0.01708	0.01767	0.01833	0.01904	0.01982
σ [$N \cdot m^{-1}$]	0.00351	0.00367	0.00377	0.00382	0.00380	0.00372

60%/40% and 50%/50%, which correspond to temperature glides of 2.49 °C, 4.43 °C, 5.60 °C, 6.33 °C and 6.54 °C respectively (Table 1). The heat transfer coefficients are determined at a condensing saturation pressure of 2.43 MPa in smooth straight tubes. At this pressure the dew point temperature for condensation will vary between 60 °C (100% R-22) and 86 °C (50% R-22) [11].

2. Test facility

A test facility was specifically constructed to measure in-tube condensation of pure refrigerants and refrigerant mixtures. The overall test facility is shown in Fig. 1. It was a vapour compression refrigeration and/or heat pump system. The compressor was a hermetically sealed, reciprocating type with an electrical consumption of approximately 3.5 kW. An oil separator was connected parallel to the compressor with a by-pass line. By manually controlling the flow through the by-pass line and through the oil separator the oil fraction in the refrigerant could be controlled. Refrigerant liquid samples were taken downstream of the after-condenser and analysed for oil concentration according to the ANSI/ASHRAE 41.4 [12] standard. For this study, full use was made of the oil separator and only results of oil concentrations less than 0.01% were used.

The test-condenser consisted of eight horizontal coaxial double tube condensers in series labelled A, B, C, up to N, where $N = 8$, as shown in Fig. 1. The inner tube of each test section was a hard-drawn refrigeration copper tube with an inner diameter of 8.11 mm and an outer diameter of 9.53 mm (3/8 inch). The thermal conductivity of the tubes was 339 $W{\cdot}m^{-1}{\cdot}{}^{\circ}C^{-1}$. Spacers were used halfway in each test section to keep the inner tubes from bending. The heat transfer length of each section was 1603 mm and the distance between pressure drop measuring points 1400 mm. The outer tube was also a hard-drawn copper tube with an inner diameter of 17.27 mm and an outer diameter of 19.05 mm (3/4 inch). Sight-glasses were installed between each test section and the following to observe the flow patterns. All test sections were well insulated with 13 mm of armoflex inside a 50 mm glass wool box to prevent heat leakage effectively. A by-pass line was connected parallel to the test-condenser to control the refrigerant mass flow through the test sections. A water-cooled after-condenser was used to ensure that only liquid refrigerant enters a coriolis mass flow meter with an error of ±0.1%. The sight-glasses before and after the coriolis flow meter was to ensure that liquid only flow through it. A filter drier followed it and a hand-

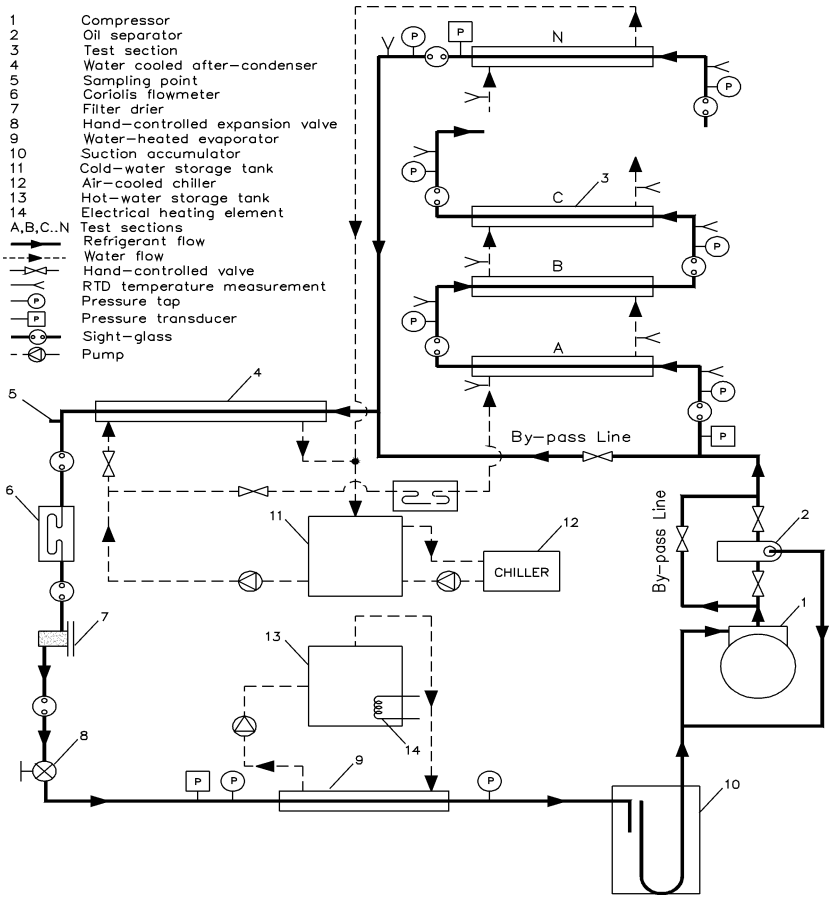

Fig. 1. Schematic of test facility.

controlled expansion valve for controlling the evaporating temperature. A water-heated evaporator was used and a suction accumulator on the low-pressure side to complete the refrigerant loop.

Two main water loops were used, one flowing through the condensing side and one flowing through the evaporating side. On the condensing side the water was kept constant at a temperature of 55 °C to 85 °C (depending on the experiments conducted) in a 1 000 litre insulated storage tank connected to a 15 kW chiller. The water flow rate through the test sections could be controlled with a hand-controlled valve. The flow rate of the water through the test sections was measured with a coriolis mass flowmeter with an error of ±0.2%. A similar flow loop was used on the evaporating side, also with an insulated 1 000 litre storage tank but connected to a 24 kW electric resistance heater. This water was also kept constant at a temperature of 8 °C to 30 °C, depending on the experiments conducted. By increasing or decreasing the temperature of the water through the evaporator, the refrigerant density at the compressor inlet and thus refrigerant mass flow could also be changed. The water temperatures in both loops could be thermostatically controlled at a constant temperature with an error of ±1 °C. As the storage capacities of the two tanks were relatively large the source and sink temperatures were very stable which helped in obtaining quick steady state conditions during experiments.

Temperatures were measured with resistance temperature devices (RTDs) calibrated to measure temperature differences with errors less than ±0.1 °C. Temperatures were measured at the locations shown in Fig. 1. At each of these locations, three RTDs were located at the top, sides and bottom of the tube to take care of any circumferential temperature variation. The average temperature of the three values was used, with the side RTD weighted double, as the average temperature measurement. Absolute pressures on the high-pressure side were measured with a 160 mm dial pressure gauge with a range of 0 to 2500 kPa. The gauge was calibrated to an error of ±5 kPa.

3. Data reduction

Annulus heat transfer coefficient. Before the test condenser was connected to the experimental set-up shown in Fig. 1, the annulus heat transfer coefficient of each section was determined individually in a water-to-water configuration. The annulus heat transfer coefficient was determined by using the modified Wilson plot technique [13]. For each test section at least 20 data points were used, all with an energy balance of less than ±2% (the average heat transfer between the inside heat transfer and outside heat transfer was used as the reference). Before the test condenser was connected into the experimental set-up it was dried with high flows of nitrogen and evacuated several times to a pressure of less than 6 Pa. Once connected and charged with R-22, it was operated for a period of 14 days during which time the refrigerant charge and filter drier were changed twice. This was to eliminate possible water moisture in the inner tube from the Wilson plot experiments before the experiments in this study were conducted.

Assuming no fouling, the heat transfer coefficient (which is the regionally average for each section) was obtained from:

$$h_\mathrm{i} = \left[\left(\frac{1}{U_\mathrm{o}} - \frac{A_\mathrm{o}\ln(R_\mathrm{o}/R_\mathrm{i})}{2\pi kL} - \frac{1}{h_\mathrm{o}}\right)\frac{A_\mathrm{i}}{A_\mathrm{o}}\right]^{-1} \tag{1}$$

The conductive resistance term was taken into consideration in Eq. (1), although the term is very small in comparison with the two convective resistance terms. The local heat transfer coefficients were integrated along the total length of the condenser using the trapezoid rule to obtain the integrated average heat transfer coefficient. The overall heat transfer coefficient was calculated from the sensible heat gain of the water and the logarithmic mean temperature difference as follows

$$Q = U_\mathrm{o}A_\mathrm{o}\Delta T_\mathrm{LMTD} \tag{2}$$

where

$$Q = m_\mathrm{w}C_\mathrm{Pw}(T_\mathrm{out,w} - T_\mathrm{in,w}) \tag{3}$$

The logarithmic temperature difference was calculated by

$$\Delta T_\mathrm{LMTD} = \frac{(T_\mathrm{r,in} - T_\mathrm{w,out}) - (T_\mathrm{r,out} - T_\mathrm{w,in})}{\ln[(T_\mathrm{r,in} - T_\mathrm{w,out})/(T_\mathrm{r,out} - T_\mathrm{w,in})]} \tag{4}$$

The first test section was balanced with the refrigerant enthalpy change to obtain the outlet enthalpy (which is also the inlet enthalpy for the next test section)

$$h_\mathrm{out,r} = h_\mathrm{in,r} - \frac{Q}{m_\mathrm{r}} \tag{5}$$

where h_in is the refrigerant inlet enthalpy for the first or second test-section obtained from a refrigerant database [11] using its inlet pressure and temperature as the inlet enthalpy was usually in the superheat region. Usually the outlet of the second test section was in the two-phase region. Then the outlet enthalpy of the second test section was used in Eq. (5) in the place of h_in. The inlet and outlet enthalpies of each test section as well as the enthalpies of saturated vapour and liquid were used to determine the inlet and outlet qualities. As the temperature and pressure were measured at the inlet of the first test section, the beginning of condensation could be determined from Eq. (5) and Eq. (6).

$$x = \frac{h_\mathrm{r} - h_\mathrm{r,f}}{h_\mathrm{r,g} - h_\mathrm{r,f}} \tag{6}$$

The average between the inlet and outlet qualities was used to determine the refrigerant quality.

For the mixtures, the Silver–Bell–Ghaly method [14] was used for mass transfer correction when theoretical predictions of the heat transfer coefficients were made which were compared with measurements.

A propagation of error analysis [15] was performed to determine the uncertainty in the measured local heat transfer

coefficients. Using this method, the uncertainty for the heat transfer coefficients was found to range from a low of ±4% at the highest heat flux to a high of ±20% at the lowest heat flux. Uncertainties in the average heat transfer coefficients ranged from ±7% to ±13% over the mass flux ranged reported.

4. Results

The results obtained for different mixtures of R-22 with R-142b are shown in Figs. 2–5. All the results are for a saturation pressure of 2.43 MPa. In Figs. 2–4, the local heat transfer coefficients are given as function of quality and in Fig. 5 the average heat transfer coefficients are given as function of mass flux. In Figs. 2–4 the mass fluxes were for 100 $kg{\cdot}m^{-2}{\cdot}s^{-1}$, 300 $kg{\cdot}m^{-2}{\cdot}s^{-1}$, and 600 $kg{\cdot}m^{-2}{\cdot}s^{-1}$. These mass fluxes correspond to observed wavy, mixed and annular flow regimes. The results were obtained for different mass fluxes from 100% R-22, decreasing with steps of 10% up to 50%/50% R-22/R-142b. The general conclusion drawn from Figs. 2–4, is that at low mass fluxes (Fig. 2) the local heat transfer coefficients are more dependent on the mass fraction of R-22/R-142b, than at higher mass fluxes (Fig. 4).

In Fig. 2 the local heat transfer coefficients for wavy flow decreased by 33% on average from 100% R-22 to 50%/50% R-22/R-142b. In Fig. 3 the flow regime changes from annular to wavy in the direction of flow. While the flow is annular (quality > 0.7), the local heat transfer coefficients are not strongly dependent on the refrigerant mass fraction. The decrease in local heat transfer coefficients from 100% R-22 to 50%/50% R-22/R-142b is on average approximately 7%. However, while in the process of changing from annular to wavy, and while in the wavy flow regime (quality < 0.5) the heat transfer coefficients are more dependent on the refrigerant mass fraction.

In the wavy regime the local heat transfer coefficients decrease on average by approximately 25% when the mass fraction decreases from 100% R-22 to 50%/50% R-22/R-142b. The visually observed change in flow regime from an annular regime to a wavy regime is at qualities between 0.58 to 0.64 for 100% R-22 and increases to between 0.63 and 0.73 for 50%/50% R-22/R-142b. The general trend is that if R-142b is added to R-22, transition from the annular regime to wavy regime happens sooner as the fraction of R-142b increases.

At higher mass fluxes (i.e., 500 $kg{\cdot}m^{-2}{\cdot}s^{-1}$ and more) the flow was visually observed to be predominately annular. The local heat transfer coefficients were also not strongly influenced by the refrigerant mass fraction, as can be observed for the mass flux of 600 $kg{\cdot}m^{-2}{\cdot}s^{-1}$, shown in Fig. 4. The average decrease in local heat transfer coefficients was only 7% as the refrigerant mass fraction changed from 100% R-22 to 50%/50% R-22/R-142b.

In Fig. 5 the average heat transfer coefficients are given as function of mass flux. For each refrigerant mass fraction,

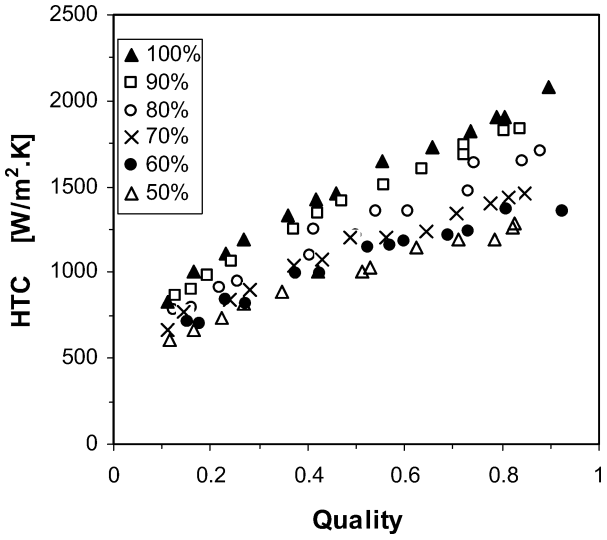

Fig. 2. Heat transfer coefficients at a mass flux of 100 $kg{\cdot}m^{-2}{\cdot}s^{-1}$ (wavy flow) at different mass fractions of R-22/R-142b. (The legends indicate the mass fraction of R-22.)

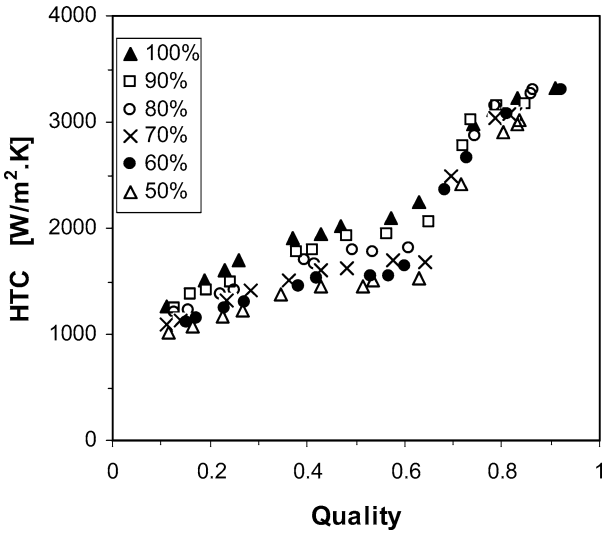

Fig. 3. Heat transfer coefficients at a mass flux of 300 $kg{\cdot}m^{-2}{\cdot}s^{-1}$ (mixed flow) at different mass fractions of R-22/R-142b. (The legends indicate the mass fraction of R-22.)

heat transfer coefficients were measured at mass fluxes of 40 $kg{\cdot}m^{-2}{\cdot}s^{-1}$ to 775 $kg{\cdot}m^{-2}{\cdot}s^{-1}$ at an average saturation pressure of 2.43 MPa. The average inlet quality was 85% and the average exiting quality was 10%. At mass fluxes between 40 $kg{\cdot}m^{-2}{\cdot}s^{-1}$ to 350 $kg{\cdot}m^{-2}{\cdot}s^{-1}$, the refrigerant mass fraction influences the average heat transfer coefficient by up to 100%. The heat transfer coefficients decrease if the mass fraction of R-22 is decreased. At mass fluxes higher than 350 $kg{\cdot}m^{-2}{\cdot}s^{-1}$, the heat transfer coefficients are not strongly influenced by refrigerant mass fraction.

As a final check on the accuracy of the measurement technique, a comparison was made off the average of the heat transfer coefficients for each data set and the measured average heat transfer coefficient determined from Eq. (1). The averages of the heat transfer coefficients for the tests are

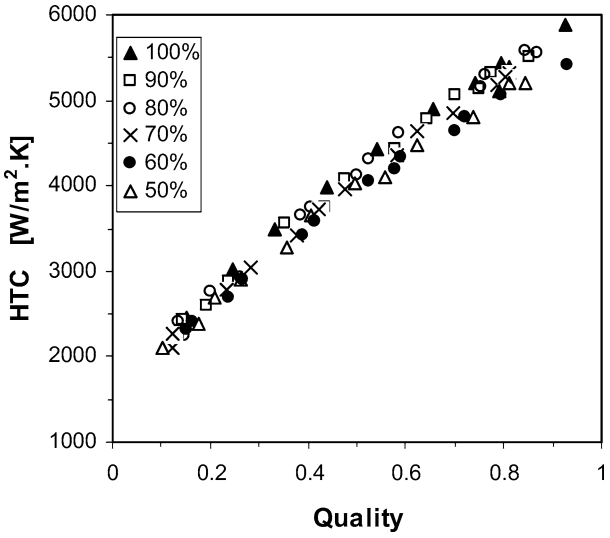

Fig. 4. Local heat transfer coefficients at a mass flux of 600 $kg{\cdot}m^{-2}{\cdot}s^{-1}$ (annular flow) at different mass fractions of R-22/R-142b. (The legends indicate the mass fraction of R-22.)

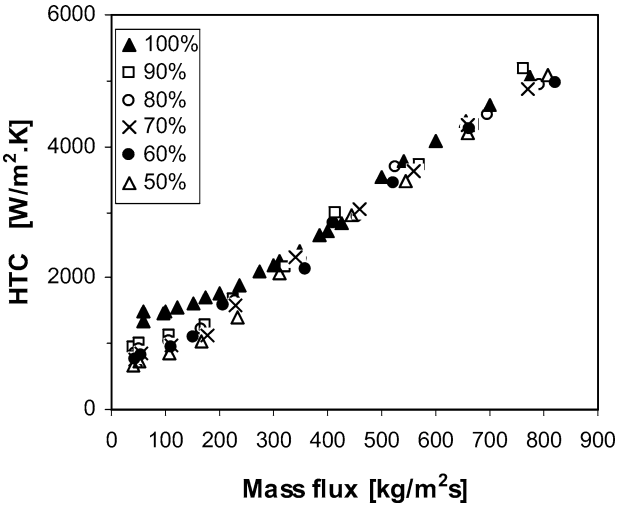

Fig. 5. Average heat transfer coefficients at a constant pressure of 2.43 MPa at different mass fractions of R-22/R-142b. (The legends indicate the mass fraction of R-22.)

determined with an area-weighted average. The agreement is good as the average error is 4% and the maximum error is 7%.

5. Conclusions

This paper presents two-phase heat transfer coefficients for condensation of R-22 and five mixture mass fractions of R-22/R-142b from 90%/10% to 50%/50%. Heat transfer coefficients were determined in an 8.11 mm inner diameter smooth tube.

Heat transfer coefficients for R-22 and the different mass fractions of R-22/R-142b were measured over a mass flux range of 40 $kg{\cdot}m^{-2}{\cdot}s^{-1}$ to 800 $kg{\cdot}m^{-2}{\cdot}s^{-1}$. At each mass flux, heat transfer coefficients were determined over the full range of qualities. It was found in general that the heat transfer coefficients decreased as the mass fraction of R-142b was increased. At low mass fluxes, between 40 $kg{\cdot}m^{-2}{\cdot}s^{-1}$ and 350 $kg{\cdot}m^{-2}{\cdot}s^{-1}$, the flow regime was observed to be predominately wavy. In this regime the average heat transfer coefficient decreased by up to a third from pure R-22 to 50%/50% R-22/R-142b. At high mass fluxes, of 350 $kg{\cdot}m^{-2}{\cdot}s^{-1}$ and more, the flow regime was predominately annular and the heat transfer coefficients decreased only with approximately 7% when the R-142b mass fraction was increased to 50%.

References

[1] H.H. Kruse, T. Tiedemann, Experience with HCF refrigerants and projections for future applications, current and projected use of refrigerants in Europe, in: ASHRAE/NIST Refrigerants Conference: Refrigerants for the 21st Century, October 6 and 7, Gaithersburg, Maryland, 1997, pp. 44–56.
[2] J.P. Meyer, G.P. Greyvenstein, Hot water for homes in South Africa, Energy Internat. J. 16 (7) (1991) 1039–1044.
[3] J.P. Meyer, G.P. Greyvenstein, Hot water for large residential units, hospitals and laundries with heat pumps in South Africa: A techno-economic analysis, Energy Convers. Management 33 (2) (1992) 135–143.
[4] F.J. Smit, J.P. Meyer, Investigation of the potential effect of zeotropic refrigerant mixture on performance of a hot-water heat pump, ASHRAE Trans., San Francisco 104 (Part 1A) (1998) 387–394.
[5] A.F.B. Johannsen, Potential of non-azeotropic refrigerant mixtures for water-heating heat pumps in South Africa, Department of Mineral and Energy Affairs, Report Nr. ED 8807, Pretoria, South Africa, 1992.
[6] F.J. Smit, The influence of a non-azeotropic refrigerant mixture on the performance of a hot-water heat pump, M. Eng. Dissertation, Rand Afrikaans University, Johannesburg, South Africa, 1996.
[7] S.A. Kebonte, Condensation heat transfer and pressure drop coefficients of R22/R142b in a water cooled helically coiled tube-in-tube heat exchanger, M. Eng. Dissertation, Rand Afrikaans University, Johannesburg, South Africa, 1999.
[8] J.M. Bukasa, Average boiling heat transfer and pressure drop coefficients of R22/R142b in a helically coiled water heated tube-in-tube heat exchanger, M. Eng. Dissertation, Rand Afrikaans University, Johannesburg, South Africa, 1999.
[9] J.P. Meyer, J.M. Bukasa, S.A. Kebonte, Average boiling and condensation heat transfer coefficients of the zeotropic refrigerant mixture R22/R142b in a coaxial tube-in-tube heat exchanger, ASME J. Heat Transfer 122 (1) (2000) 186–188.
[10] M. Shizuyo, M. Itoh, K. Hijrkata, Condensation of nonazeotropic binary refrigerant mixtures including R-22 as a more volatile component inside a horizontal tube, ASME J. Heat Transfer 117 (1995) 538–543.
[11] NIST, Thermodynamic and transport properties of refrigerants and refrigerant mixtures database (REFPROP Ver. 6.01), Gaithersburg, MD: National Institute of Standards and Technology, 1998.
[12] ANSI/ASHRA, ASHRAE STANDARD 41.4, Standard method for measurement of proportion of lubricant in liquid refrigerant, American Society of Heating, Refrigerating and Air-Conditioning Engineers, Atlanta, GA, 1996.
[13] D. Briggs, E. Young, Modified Wilson plot technique for obtaining heat transfer correlations for shell and tube heat exchangers, Chemical Engrg. Progress Sympos. 65 (2) (1969) 35–45.
[14] R.S. Silver, An approach to a general theory of surface condensers, Proc. Inst. Mech. Engrs., Part 1 179 (14) (1964) 339–376.
[15] S. Kline, F. McClintock, Describing uncertainties in single-sample experiments, Mech. Engrg. 75 (1953) 3–8.